Have coastal embankments reduced flooding in Bangladesh?

Mohammed Sarfaraz Gani Adnan [a,b],*, Anisul Haque [c], Jim W. Hall [a]

[a] *Environmental Change Institute, School of Geography and the Environment, University of Oxford, South Parks Road, OX13QY Oxford, United Kingdom*

[b] *Department of Urban & Regional Planning, Chittagong University of Engineering and Technology (CUET), Chittagong, 4349, Bangladesh*

[c] *Institute of Water and Flood Management, Bangladesh University of Engineering and Technology (BUET), Bangladesh*

Abstract[1]

From the 1960s, embankments have been constructed in south western coastal region of Bangladesh to provide protection against flooding, but the success of the polder programme is disputed. We present analysis of floods during the years 1988-2012, diagnosing whether the floods were attributable to monsoonal precipitation (pluvial flooding), high upstream river discharge into the tidal delta (fluvio-tidal flooding), or cyclone-induced storm surges. We find that pluvial flooding was the most frequent, but typically resulted in less flooded area (11.44% of the region on average) compared with the other forms of flooding. The greatest area of inundation (48% of total area) occurring in 2001 as a consequence of fluvio-tidal and surge flooding, whilst cyclone Sidr in 2007 flooded 35% of the area. We modelled these different forms of inundation to estimate what flooding might have been had the polders not been constructed. For the 'no embankment' counter-factual scenario, our model demonstrated that because of a combination of subsidence and inadequate drainage, construction of the polders has increased the pluvial flooded area by 6.5% on average (334 km^2). However, during the 1998 fluvio-tidal flood, the embankments protected an estimated 54% of the area from flooding. During the cyclone Sidr storm surge event, embankment failure in several polders and pluvial inundation resulted in 35% area inundation, otherwise, the total inundation would have been 18% area. We conclude that whilst polders have provided protection against storm surges and fluvio-tidal events of moderate severity, they have exacerbated more frequent pluvial flooding and promoted potential flooding impacts during the most extreme storm surges.

Key words: Bangladesh coastal embankment; extreme events; flood classification; pluvial flood; fluvio-tidal flood; storm surge flood

[1] https://doi.org/10.1016/j.scitotenv.2019.05.048

1. Introduction

Structural flood defence systems are one response to flood hazards (Bamberg et al., 2017). While embankments, levees and dikes usually provide flood protection up to a given severity of flooding, these structures are costly and may exacerbate flooding under some circumstances, as well as potentially encouraging the build-up of exposed people and assets (Hui et al., 2016).

Due to the deltaic geographical setting and high population density, Bangladesh is well-known as being vulnerable to flooding (Islam et al., 2016b; Moniruzzaman, 2012). The coastal region is subject to multiple flood hazards, including pluvial floods, which are inundations induced by monsoon precipitation, fluvio-tidal floods and storm surge-induced floods (Abedin and Shaw, 2015; Alam et al., 2017; Brouwer et al., 2007; Haque et al., 2018; Islam et al., 2016a). The impact of several catastrophic floods impelled the Bangladesh government to construct coastal embankments in the 1960s to protect agricultural land and communities (Nishat et al., 2010; Paul and Rashid, 2017; Rahman and Salehin, 2013). Coastal embankments have compartmentalized a portion of coastal region into polders. Their construction was accompanied by the excavation of drainage channels and sluice gates to impede salt water intrusion in the dry season, drain excessive rain water, and allow fresh river water flow to polders in the wet season for irrigation purposes (Masud et al., 2018).

The coastal embankment programme had a profound influence on the geomorphology of the coastal zone, as well as contributing to a transformation in human settlement patterns. The embanked region experienced rapid land use change (Abdullah et al., 2019; Akber et al., 2018). In the last couple of decades, a substantial growth in shrimp farming, replacing agricultural lands, is reportedly associated with soil salinity promoted by the intrusion of saline water in polders (Mukhopadhyay et al., 2018). Moreover, storm surges and pluvial flooding inundated agricultural lands, which has been reflected in a net reduction in land use for

agriculture (Khan et al., 2015). In this naturally dynamic sediment system, reducing flow in the channels of the delta, due to the separation of upstream river 'Mathabhanga' from the river Ganges, caused siltation in the riverbed (Alam et al., 2017). Polders simultaneously also impeded sedimentation within embanked region and resulted in land subsidence inside the polders (Auerbach et al., 2015). As a result of reduced sediment supply or irregular sedimentation, compaction of sediment, and anthropogenic activities (e.g. shrimp farming) (Brammer, 2014; Brown and Nicholls, 2015), the coastal region on average experienced about 2-3 mm/year of land subsidence (Brown and Nicholls, 2015). In addition, physical deterioration and unreliable operation of the sluice gates caused prolonged inundation during the monsoon period (Auerbach et al., 2015; Choudhury et al., 2004; Van Staveren et al., 2017). The earthen embankments are subject to riverbank erosion which can breach the polders, a process that can be exacerbated by tropical cyclones and lead to extensive flood damage (Bhuiyan and Dutta, 2012; Haque and Nicholls, 2018). The polders have also been criticized for their impact on coastal habitats and ecology (Roy et al., 2017).

Though these criticisms of polderization are widely reported (Alam et al., 2017; Auerbach et al., 2015; Tareq et al., 2018), it has proved difficult to provide quantified evidence of the effect of the coastal embankment programme because (i) the flooding processes are complex and derive from many sources and (ii) it is difficult to establish what the extent and severity of flooding might have been had the coastal embankments not been constructed. This paper seeks to address both of these challenges by (i) analysing past events to diagnose different types flooding and (ii) estimating the extent of flooding that could have occurred had the polders not been constructed. The first challenge is addressed through empirical analysis of the hydrometeorological factors that can explain the severity of observed floods, whilst the second is tackled by constructing models of different types of flooding.

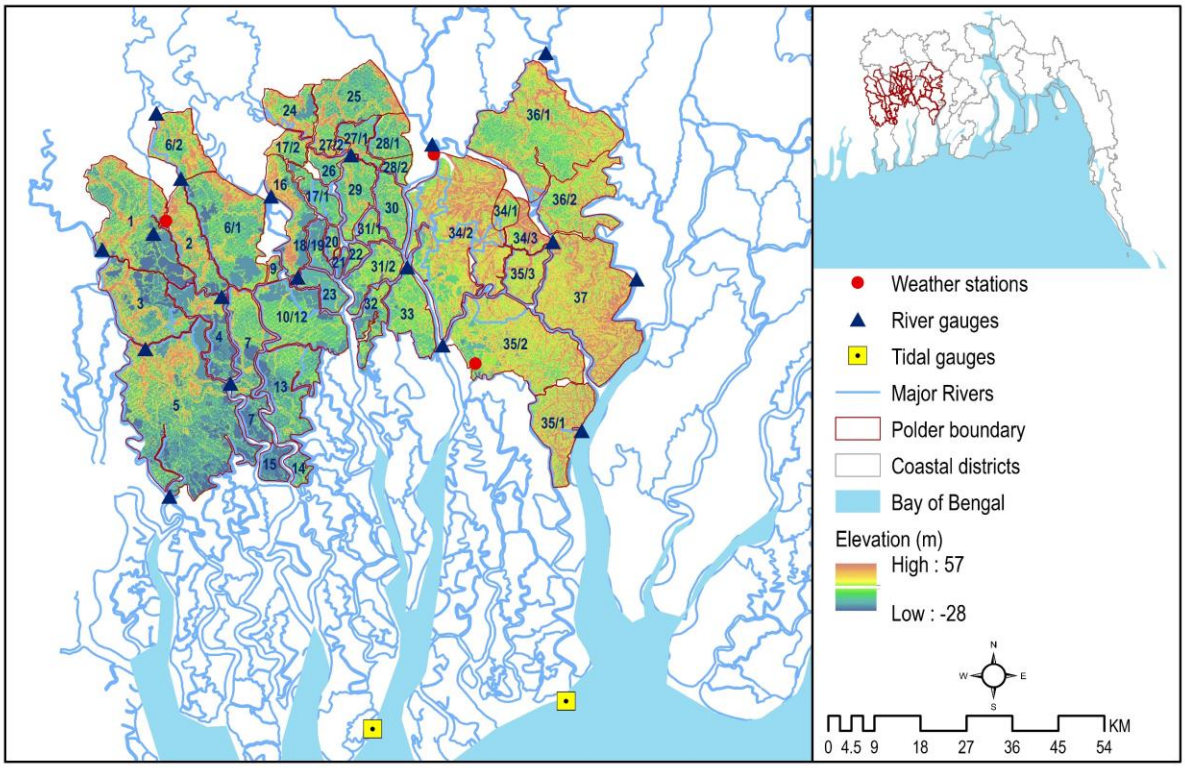

Fig. 1. South western embanked region of Bangladesh.

2. Materials and methods

This research was conducted in two stages (Fig. 2). First, a series of flood observations for the years 1988-2012 were obtained from remote sensing imagery. Records of rainfall, river water level, and surge levels for the same period were used to identify the main type of flooding for each observed event. Second, the counter-factual scenario without the construction of coastal embankments was modelled in order to hypothesise how the flooding might have been different without the polders.

2.1. Flood hazard of south western coastal region of Bangladesh

The study addresses the south western coastal region of Bangladesh (Fig. 1) which is vulnerable to fluvio-tidal flooding, monsoonal precipitation induced pluvial flooding, and storm surges (Bhuiyan and Dutta, 2012; Gain et al., 2017). In the dry season, tidal oscillations dominate the low flows in the river channel in this region, making it susceptible to salt water intrusion. Before polder construction, a common practice from local people was to build

temporary earthen embankments in the dry season to protect the land from salinity and remove those in wet season to enable sedimentation. Starting in 1960 a total of 44 polders were built in the Coastal Embankment Project (CEP) (Nowreen et al., 2014; Paul and Rashid, 2017), protecting 5187km^2 (WARPO, 2018). Polder construction transformed the coastal region into an agriculturally productive zone and encouraged people to settle within the polders (Nowreen et al., 2014). Conversely, polder construction de-linked the floodplain (Talchabhadel et al., 2016) and induced several problems including river flow reduction, siltation in tidal channels, drainage congestion, waterlogging, land subsidence, polder breaching, soil salinity, etc. (Auerbach et al., 2015; Choudhury et al., 2004; Gain et al., 2017; Nowreen et al., 2014; Paul and Rashid, 2017). For instance, polder construction has resulted in 1.0-1.5m of land subsidence inside an embanked area (Polder 32), whereas the outside of this embankment, the neighbouring Sundarban mangrove forest, has remained comparatively unchanged (Auerbach et al., 2015).

In response to multifaceted problems related to polders, over the years the government of Bangladesh, in cooperation with various international donor agencies, have implemented several projects. The World Bank, who supported the CEP project, has started the Coastal Embankment Improvement Project (CEIP) Phase I in 2015, which is rehabilitating and/or reconstructing several polders, as well as upgrading the drainage channels and structures (Paul and Rashid, 2017). Meanwhile, the Blue Gold project, funded by Government of the Netherlands (GoN) and operated by the Bangladesh Water Development Board (BWDB), has been responsible for rehabilitation of water control structures within 26 polders districts (http://www.bluegoldbd.org/). In addition, Tidal River Management (TRM) has been adopted in an attempt to restore sedimentation within the polders through selective flooding (Van Staveren et al., 2017), gaining attention as a potential alternative to structural flood protection (Gain et al., 2017). The idea of TRM is to allow river flow into low-lying bowl-shaped

depressions (termed as ‘Beel’) within polder for sediment deposition to fill those depressions (Masud et al., 2018; Van Staveren et al., 2017). Though historically a community driven approach, BWDB implemented TRM in several ‘Beels’ in 1991-2013 (Masud et al., 2018). Despite several initiatives, the challenges of providing sustainable flood risk management in the south western polder region are intensifying, with the threat of sea level rise, upstream modification of river flows and sediments from the Ganges Brahmaputra Meghna river system, and high population density providing little space for adaptation (Haque et al., 2018; Kay et al., 2018).

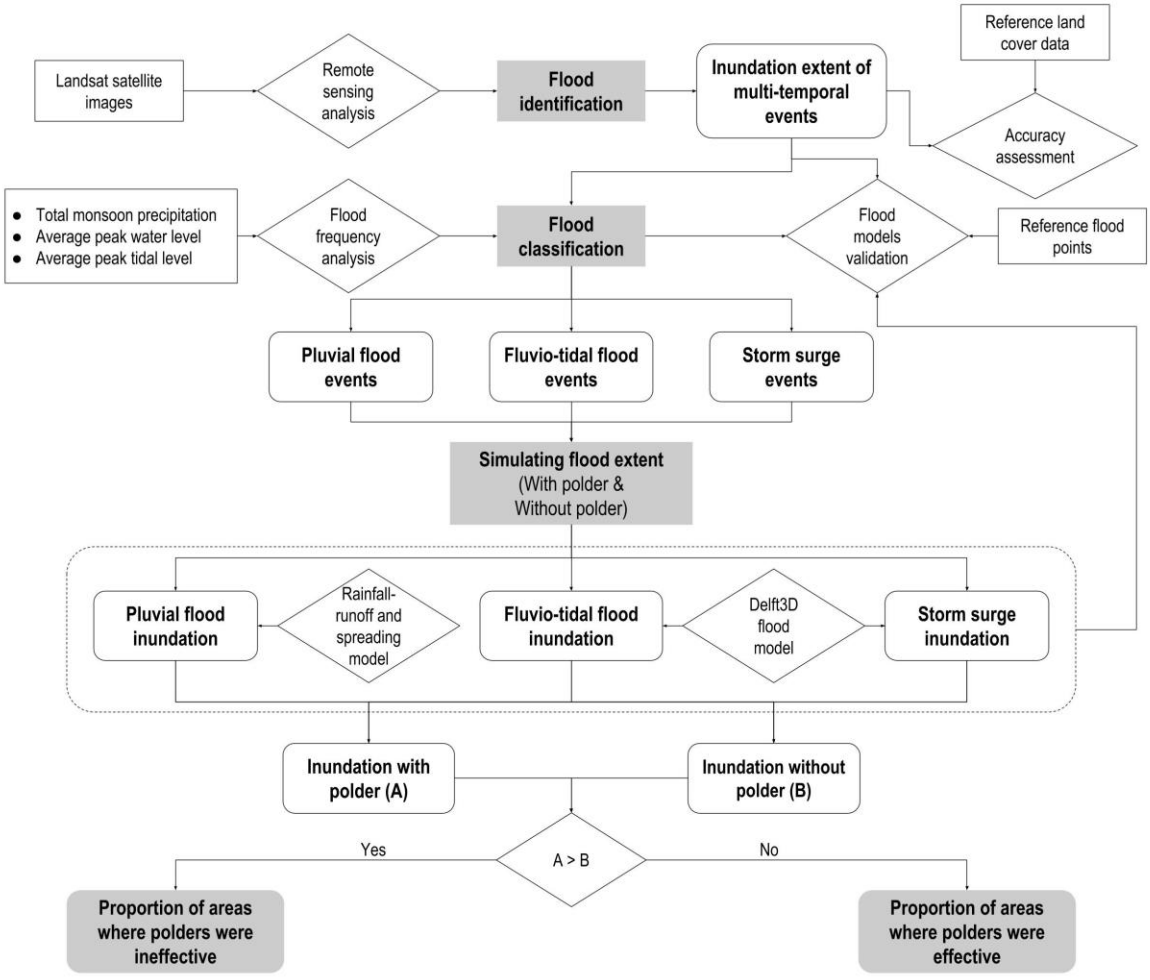

Fig. 2. Analytical process of this study.

2.2. Identifying flood events

In last two decades (Hoque et al., 2011), water surface detection through remote sensing techniques has become an essential tool for various disciplines (Sanyal and Lu, 2004; Sarp and Ozcelik, 2017). Among various methods, water-indexing techniques have proved to be very useful for quick flood detection (Sarp and Ozcelik, 2017). This study applied the Modified Normalized Difference Water Index (MNDWI) (Xu, 2006) using ArcGIS 10.6.1 to detect water surfaces during pre (dry) and post (wet) monsoon period in a year. MNDWI uses green and middle infrared (MIR) bands of Landsat satellite images. It generates positive values for water surfaces and negative values for built-up areas, soil surfaces and vegetation. Then a change detection algorithm was used in Geographic Information System (GIS) to identify cells that changed from being normally dry to wet, which were classified as flood cells for that year. Cloud cover during the monsoon period (May to September) (Ahmed and Akter, 2017) meant that the analysis was applied to compare pre and post monsoon images. The image database is summarised in Table S2 of the Supplementary Information.

The major cyclone Sidr in 2007 caused prolonged flooding within the polders (Tareq et al., 2018), which lasted into 2008. Hence using pre-monsoon images of 2008 could cause under estimation of flood extent in 2008, so dry season images from 2007 we employed to detect flood extent in both 2007 and 2008.

The accuracy of MNDWI based classified images was assessed, for three different years (1989, 2001, and 2010), against reference land cover data (classified and validated images) collected from Mukhopadhyay et al. (2018) (Table S1, supplementary document), producing an error matrix to estimate the overall accuracy and kappa statistics. The overall accuracy depicts a percentage agreement of pixels correctly classified (Lillesand et al., 2014). The kappa statistics (κ) is a measure for inter-rater reliability testing, whose value can range from -1 to +1, where 'values ≤ 0 as indicating no agreement and 0.01–0.20 as none to slight, 0.21–0.40

as fair, 0.41– 0.60 as moderate, 0.61–0.80 as substantial, and 0.81–1.00 as almost perfect agreement' (McHugh, 2012). The reference land cover data were converted into binary images (water, dry) and classified dry season (pre-monsoon) images of those three years were employed to estimate the indices of classification consistency. In this study, 'substantial agreement' within pixels between reference and classified land cover images were found for 1989 and 2010, and 'almost perfect agreement' was achieved for 2001 image classification (Table S3, supplementary document). The processed flood maps were used to estimate the severity of observed flooding and also to validate the flood simulation outputs in the second phase of the study. The reference land cover maps included 12 land use classes, in which general waterbodies are separated from aquaculture, mixed agriculture/aquaculture and agricultural lands. These maps were further used to analyse the types of land uses exposed to pluvial flooding.

2.3. Flood event classification

To attribute the observed floods to different sources of flooding, we analysed the severity of monsoon rainfall and elevated water levels within the region. Extreme value analysis was conducted by fitting to a generalized extreme-value (GEV) distribution using the L-moment method (Coles et al., 2001; Gilleland and Katz, 2016). The cumulative distribution function of the GEV distribution is:

$$G(z) = \exp\left[-\left\{1 + \varepsilon\left(\frac{z-\mu}{\sigma}\right)\right\}_{+1}^{-1/\varepsilon}\right] \quad (1)$$

Where, z is the random variable (monsoon precipitation/peak river water level/peak surge level) and ε, μ, and σ are the shape, location, and scale parameters respectively. The return period (T) was estimated by following formula:

$$T = \frac{1}{1 - G(z)} \quad (2)$$

The precipitation frequency analysis was based on 10-days gridded precipitation data from the Bangladesh Meteorological Department, aggregated into yearly monsoonal total

precipitation and computed the regional average from 1948-2012. Fluvio-tidal flood attribution was based on annual peak water level (Rao and Hamed, 2000), averaged across 18 river gauges. Finally, tidal surges were identified though analysis of peak tidal water level averaged across two tidal gauges in the Bay of Bengal, i.e. Hiron point and Khepupara (Fig. 1). Data used for flood frequency analysis are summarised in Table S1 of supplementary document.

In each year the return period of pluvial rainfall, fluvio-tidal water level and surge water level were estimated according to Equation 2, denoted T_p, T_f and T_s, respectively. We then sought to classify each year, estimating thresholds T_p', T_f' and T_s' above which a flood of the given type was said to have occurred and a flooded area A_f' which represented the threshold between 'flood' and 'non-flood' events. The thresholds were optimised according to the following criteria, applied in this order of priority:

1. The separation between 'flood' and 'non-flood' events should not be contradictory i.e. events cannot be classified as being a version of 'flood' (i.e. pluvial, fluvio-tidal or surge) and 'non-flood'.
2. If an event with multiple types flood is identified, the classification of flood event should be consistent with the ordering of severity of T, i.e. the classification should be of the event type with the greatest T.
3. All events with above average flooded area should be classified as a version of 'flood'.
4. The number of multiple classifications should be minimised.

If it is not possible to meet criteria 1-3 the number of constraint violations should be minimised.

2.4. Modelling flood events

2.4.1. Pluvial flood model

To simulate the effect of polders on pluvial flood severity, a simple pluvial flood rainfall-runoff and spreading model was established. The model was then adjusted to simulate the effects of subsidence and drainage system.

Pluvial flooding materialises based on the interaction between precipitation, evapotranspiration, surface flow, local topography and drainage. It can occur either due to intense downpours (Falconer et al., 2009; Houston et al., 2011) or by prolonged moderate to heavy rainfall (Falconer et al., 2009). In low-lying areas like the polder region of south western Bangladesh, these processes are extremely complex, so we have developed simplified GIS-based water balance and flood spreading model to estimate inundated areas.

The Thornthwaite and Mather (TM) water balance model was used to produce monthly excess precipitation grids. The water balance model takes gridded monthly total precipitation (*P*), monthly mean temperature, monthly mean daylight hours, soil texture to estimate monthly potential evapotranspiration (equation 3), monthly water deficit or excess precipitation, actual evapotranspiration (equation 4, 5, 6, 7), and excess precipitation (equation 8, 9, 10). Raster layers of potential evapotranspiration (PE) and monthly water deficit or surplus (P-PE) in mm were calculated as follows:

$$PE_m = 16\ C \left(10\frac{T}{I}\right)^a \quad (3)$$

Where, T is the monthly average temperature (˚C), I is the annual heat index for the year in concern, calculated as $I = \sum_1^{12} i$, where the monthly heat index $i = [T/5]^{1.514}$, $a = 6.75\times10^{-7}I^3 - 7.71\times10^{-5}I^2 + 1.792\times10^{-2}I + 0.49239$; the correction factor $C = m/30.d/12$, where m is the number of days in the month and d is the monthly mean daylight hours (Singh et al., 2004). The estimated monthly PE was then subtracted from the monthly P to find out the water excess (+) or deficit (-). After that, the soil budget was estimated to find the actual

evapotranspiration. At this stage, a raster layer of available water capacity ($SOIL_{max}$) was created following Thornthwaite and Mather (1957) principles. As Dingman (2002) demonstrated,

If $P_m \geq PE_m$

$$SOIL_m = min\{[(P_m - PE_m) + SOIL_{m-1}], SOIL_{max}\} \quad (4)$$

$$AET_m = PE_m \quad (5)$$

If $P_m < PE_m$,

$$SOIL_m = SOIL_{m-1}\left[exp\left(\frac{P_m - PE_m}{SOIL_{max}}\right)\right] \quad (6)$$

$$AET_m = P_m + SOIL_{m-1} - SOIL_m \quad (7)$$

Where, AET_m is the actual evapotranspiration of the month in concern; $SOIL_{m-1}$ is the soil moisture content of previous month. To solve this recursive equation, the GIS toolset started running from the first month (when P-PE <0) after the monsoon, considering that the soil moisture storage in previous month (last month of monsoon) was full, i.e. equal to the estimated available water capacity. Next, the following conditions and equations were followed to estimate the monthly and monsoonal total excess precipitation (SUR).

If $(P\text{-}PE)_m<0$,

$$\mathrm{SUR_m} = 0 \quad (8)$$

If $(P\text{-}PE)_m \geq 0$ and $SOIL_m=SOIL_{max}$,

$$\mathrm{SUR_m} = (\mathrm{P} - \mathrm{PE})_\mathrm{m} \quad (9)$$

If $(P\text{-}PE)_m \geq 0$ and $SOIL_m \neq SOIL_{max}$,

$$\mathrm{SUR_m} = (\mathrm{P} - \mathrm{AET})_\mathrm{m} + \mathrm{SOIL_m} \quad (10)$$

Monsoon total excess precipitation,

$$\mathrm{SUR_Y} = \sum \mathrm{SUR_{May\ to\ September}} \quad (11)$$

The flood extent was estimated by considering a series of surface depressions, whose catchments are nested (Diaz-Nieto et al., 2011). The SRTM DEM was analysed to identify surface depressions, their exit points (points through which water will pass to next level depressions when a depression is full), and catchment areas. While identifying exit points, the model followed the single-direction flow algorithm (D8), where one cell routed into the next steepest of eight neighbouring cells (Seibert and McGlynn, 2007), and eliminated cells which drained back to the same depression. After that it selected depression points to define respective

depressions catchments and nest levels were assigned for depression catchments. The total volume of monsoon excess water from the water balance model was assigned to each depression. The water accumulation algorithm (equation 12) was started from the highest nest level depressions to accumulate water and subsequently passes to next level depressions. At this point, the model routes additional water, after filling previous level depressions (if remains), to the existing catchment(s). This iterative process continued until the model distributed water to the lowest nest level (Diaz-Nieto et al., 2011):

$$P_{P=0 \rightarrow P<0} = \sum P_{j=1,n} + E - V \quad (12)$$

Where, P = water volume passed down from depression, E = access volume after filling the depression, V = depression volume, j = counter of nested depressions from 1 to n.

For each year (1988-2012), the model was used to simulate pluvial inundation with and without polders. For pluvial inundation 'with' polders the observed DEM was used. Drainage from the polder was constrained due to inadequate maintenance of drainage channels and deterioration of sluice gates.

Brown and Nicholls (2015) documented 205 points measurements of net subsidence. Yearly land subsidence rates used in this study ranging from 0.24mm to 10mm per year. Using these point measurements, a raster of yearly subsidence rate was created, using Inverse Distance Weighted (IDW) interpolation. Multiplying this raster with subsequent number of years starting from 1960 (commencing year of polder construction) was added to the existing DEM to reconstruct past land elevations. The reconstructed DEM was used to delineate potential flood locations (surface depressions) in the 'without' polder scenario. The estimated total excess precipitation in each year was accumulated in the depressions and nested catchments. We further developed a scenario in which drainage channels within the polders

were effectively maintained. These channels were identified by hand from the satellite image. Catchments that contained these channels were permitted to drain.

We performed sensitivity analyses for (a) the method used to interpolate land subsidence rate (b) the rate of land subsidence, which was used to establish pluvial flood model for the counterfactual scenario. First, using the observed land subsidence data we generated three additional layers of land subsidence rates, applying kriging, spline, and natural neighbour methods in GIS (Childs, 2004). These layers were incorporated to generate pluvial flood inundation simulations for the 25 years studied for the counterfactual scenario. We tested for significant differences in annual pluvial inundation in the counterfactual scenario (Figure S1, supplementary document). This was done applying one-way analysis of variance (ANOVA) test. An ANOVA test could be performed to measure the sensitivity of input parameters (e.g. DEM) in hydraulic modelling and floodplain mapping (Raber et al., 2007). The estimated *p*-value 0.22 indicated that the difference in inundation for four types of land subsidence rates is not significant. The insignificant p-value and a smaller value of F-ratio than the critical F-ratio (Table S4, supplementary document) confirmed the absence of sensitivity in the pluvial flood model in relation to method applied to interpolate the rate of land subsidence.

In addition, we generated raster layers of two land subsidence rates, randomly splitting the observed 205 points measurements of net subsidence rate into two groups. The first group contained a subset of 70% points, whereas the second group was comprised of the remaining 30% points. Yearly land subsidence rates in the two groups ranging from 1mm to 10mm and 1mm to 6mm, respectively. We applied IDW interpolation method to obtain two layers of subsidence rates, which were added (multiplying by the difference of modelled year from 1960) separately on the existing DEM to generate two different surfaces. We incorporated these surfaces in pluvial flood model to estimate the inundated area across delineated depressions. Here, we modelled the pluvial events of 2004 and 2006, when a higher amount of excess

precipitation was estimated (Fig. 6). Figure S2 in supplementary document exhibits a similar pattern of individual depression behaviour for a change in land subsidence rate. Again, ANOVA test was performed to analyse the difference in inundation during two events in individual depression, for different rates of land subsidence. The obtained p-value 0.27 and F-ratio 1.3 (< critical F-ratio 2.01) indicated that the difference in inundation in different depressions insignificant.

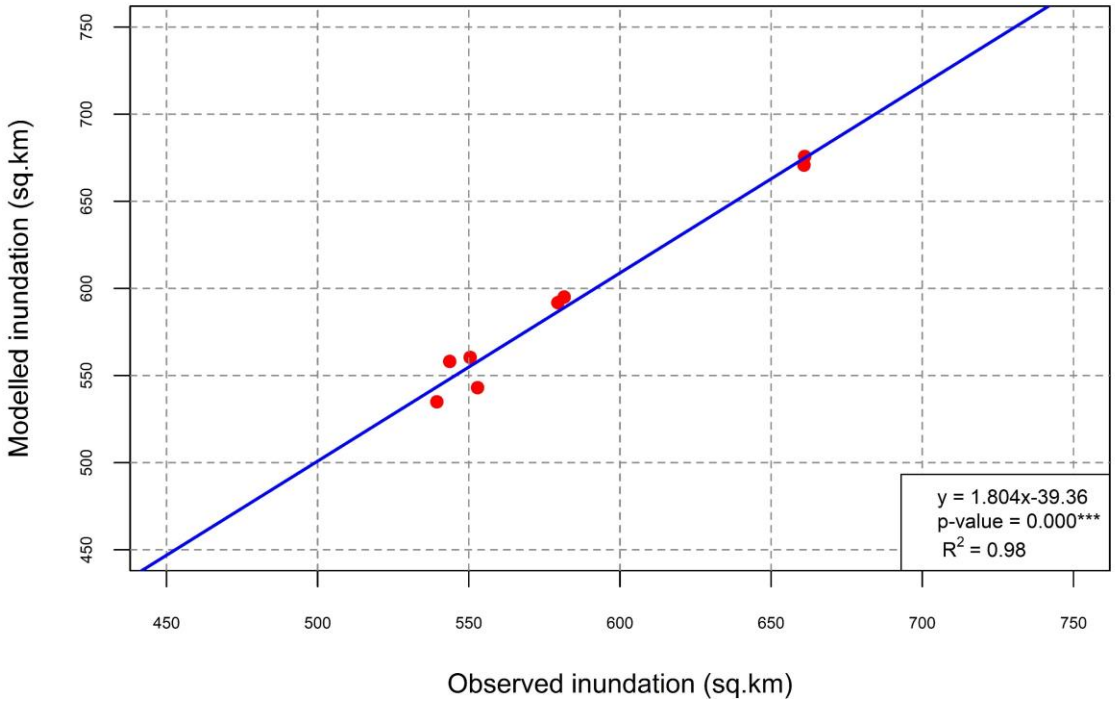

Fig. 3. Modelled versus observed pluvial flood inundation plot.

The pluvial flood model was validated based on a field survey that was conducted on May 2018 to collect GPS locations of pluvial floods and non-floods (Figure S3, supplementary document). An error matrix was produced (Table S5, supplementary document) to verify the accuracy of modelled potential flood/non-flood pixels, comparing to observations. An overall accuracy of 95% and spatial statistical κ statistics value 0.87 suggest an 'almost perfect agreement' (McHugh, 2012) between observed and modelled flood pixels.

The observed total inundation in years that were identified as pluvial flood events were plotted against the modelled inundation of corresponding years for 'with polder' scenario, yielding a coefficient of determination R^2=0.98 (Fig. 3). However, the validation process also included 2005 event, despite it was classified as 'no flood' event. The reason for using this event to validate the pluvial flood model is explained in Section 3.3.

2.4.2. Fluvio-tidal and storm surge inundation model

The Delft 3D hydrodynamic model (Haque et al., 2018) was used to estimate inundation extent from fluvio-tidal (1998) and storm surge flooding (2007) for 'with' and 'without' polder scenarios. The model domain was bounded by border with India in the west (type of boundary is not fixed), Lower Meghna estuary in the east, three major rivers (Ganges, Brahmaputra and Upper Meghna) in the north and Bay of Bengal in the south. The discretized model domain contains 896,603 grid points, where grid size varies from 186m to 1704m. Coarser grid size is provided in the ocean and finer grid size is provided in the river channels to capture the details of the river/estuarine systems and topographic variation. The model was set up for all rivers and estuaries with a width of at least 100m. Measured flow data was provided from BWDB for three the major rivers, from which fluvial flow enters the model. In absence of measured sea level data, the model takes simulated sea level data from the GCOMS model (Kay et al., 2015), which generated the tidal (ocean) boundary. As morphological changes were considered static (except subsidence) – no additional sediment input is provided. A rate of 2.6 mm/yr (Brown and Nicholls, 2015) of subsidence is considered in the area bounded by the polders including the polder itself. A DEM with a spatial resolution of 50m was provided by WARPO (2018). The ocean bathymetry data was obtained from General Bathymetric Chart of the Oceans (GEBCO) while river bathymetry data was collected from BWDB at 294 locations in coastal rivers/estuaries. Channel planforms were assumed to remain the same over the model

simulation period. Similar assumption was made for channel bed level and floodplain levels of rivers / estuaries.

The model indirectly considered impacts of land use and land cover through resistance in the floodplain. Different resistance values were specified for sea, rivers/estuaries, floodplain and forest (Sundarban). These resistance values were determined during model calibration. The calibrated Manning's roughness coefficient was spatially variable having values of 0.00025 in the ocean (considered as large water body), 0.015 to 0.025 in rivers /estuaries (a value generally considered to be valid for rivers / estuaries in the region), 0.025 to 0.040 in the floodplain, and 0.08 to 0.1 in forests including mangrove and natural plantation. The model simulated 103 polder areas (out of 139) using design heights of embankments collected from BWDB. Present day observations are only available for 61 polders (some of which are outside the study region) that show that actual polder heights can vary from 3m to 7m (Huq et al., 2010). Where actual embankment heights are not available, an average design embankment height of 4.75m is used in the model (CEIP, 2013). Storm surge modelling was based on a reconstructed cyclone track for the 2007 cyclone Sidr (Figure S4, supplementary document) that passed by the study area. Consideration of reconstructed cyclone track was based on the premise that modelled result could ideally explain the observed flood inundation. Resulting simulated inundation data was masked for the south western polder region. Further details on model setup, calibration, and validation can be found in Haque et al. (2018) and Haque and Rahman (2016).

3. Results and discussion

3.1. Identification of flood events

In 25 observed years, the inundated area ranged from 6% (in 2010) to 48% (in 2001). The mean flood footprint was 13% of the total embanked region. The patterns of inundation were heterogeneous spatially and temporally, with different parts of the embanked region flooded in different years. Six polders were flooded by more than 13% (average flood area) of

their respective area, on average. The largest extent of inundation occurred in polder 34/1, whereas the polder 28/2 and 30 experienced the lowest level of inundation (Figure S5, supplementary document).

Fig. 7(a) shows a typical inundation footprint for the year 2004 obtained from remote sensing data analysis. Here, major inundation occurred in the northern segment of embanked region. Generally, flooding in the south western part of the region was less frequent and the extent of inundation in that segment was relatively low during various events.

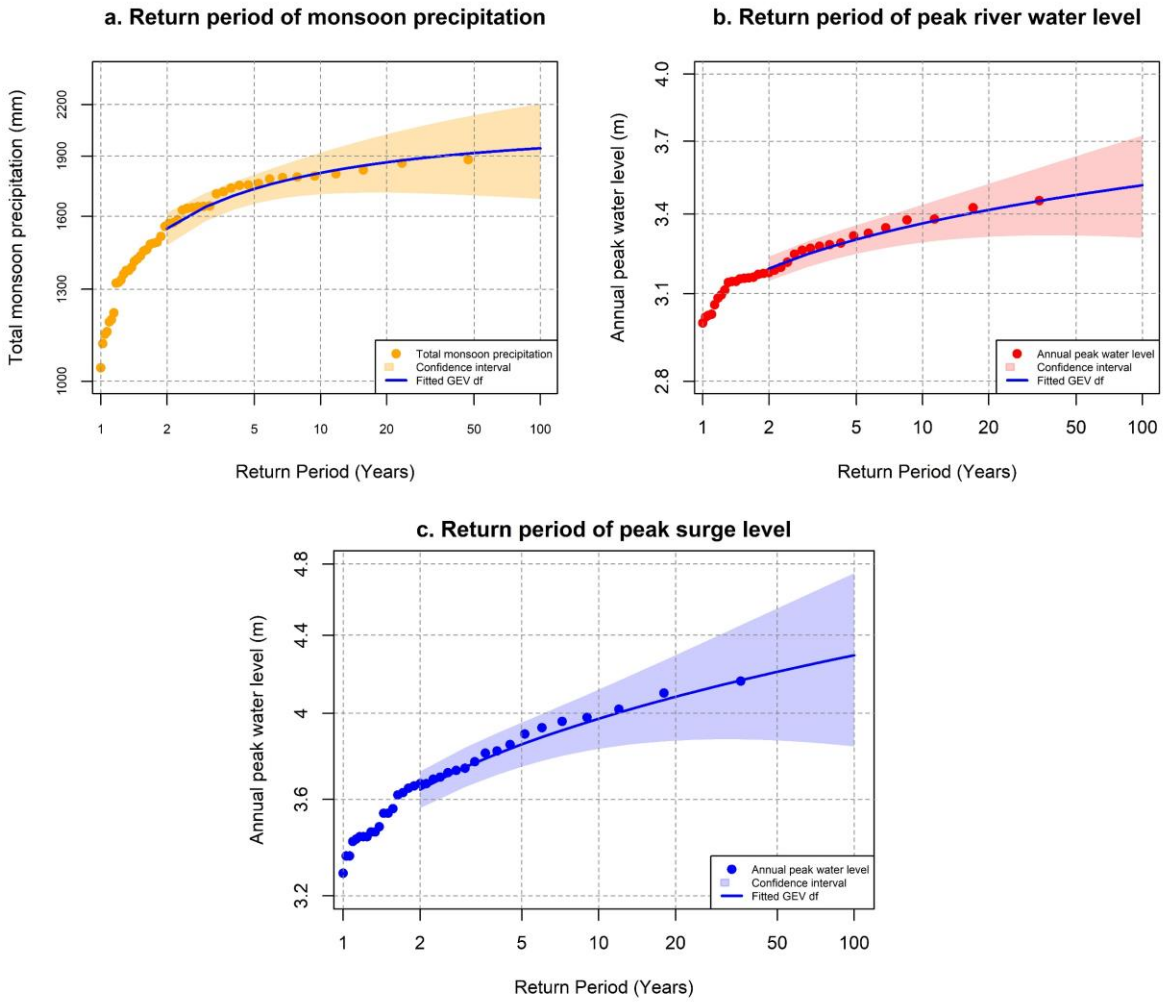

Fig. 4. Return level plots with fitted GEV df and 95% confidence bands.

3.2. Classification of flood events

3.2.1. Frequency analysis

Fig. 4 portrays the frequency analysis of total monsoon precipitation, peak river water level, and peak surge level respectively to classify them into pluvial, fluvio-tidal, and surge induced floods. The estimated return periods of these three hydrological parameters varied annually, indicating different types of floods in different years. For instance, within 25 observed years, the highest monsoon precipitation was in 2002, whereas the highest peak river water level and surge level were in 1996 and 2007 respectively. The relationship between flood conditioning factors and flood type is complex (Nied et al., 2014), in this study, we provide a simplified flood classification system estimating minimum thresholds T_p', T_f' and T_s'.

3.2.2. Flood event classification

Table 1 presents the return period of each type of flood in each year. The optimisation of return periods of three hydrological parameters yielded the following minimum flood thresholds: T_p' = 5.2 years, T_f' = 5.9 years and T_s' = 7.9 years and threshold between 'flood' and 'non-flood' events was 10.3% of the area. According to this criterion, floods were identified as occurring in 14 different years and three compound events were detected. The estimated thresholds generated one false negative and one false positive flood event. The event in 1996 was classified as 'F' even though the flood area was 9.2%. The highest T_f during that event was responsible for such attribution. Besides, 2005 event was classified as 'N' despite about 11.5% area was inundated. In 2005, the region received a lower level of monsoon precipitation, in addition to low peak river water level and surge level. The outcome of pluvial flood model explained the reason for a higher level of inundation in 2005 (Section 4.3).

We find that pluvial flooding was the most frequent, but typically resulted in less flooded area (11.4% of the region on average) compared with the other forms of flooding. The fluvio-tidal and surge induced floods caused more extensive inundation than the pluvial floods:

21.8% and 30.2% on average, respectively. The greatest area of inundation (48% of total area) occurring in 2001 as a consequence of fluvio-tidal and surge flooding, whilst cyclone Sidr in 2007 flooded 35% of the area.

Table 1. Flood attribution in south western polder region

Year	Precipitation return period (T_p)	Return period of peak river water level (T_f)	Surge peak return period (T_s)	Percentage of area inundated (A_f)	Flood type (P-Pluvial, F-Fluvio-tidal, S-Surge, N-No flood)
1988	9.5	3.9	6.5	10.3	P
1989	1.4	1.5	2.7	6.5	N
1990	2.1	2.1	2.4	9.3	N
1991	1.7	1.6	1.9	8.2	N
1992	1.3	3.4	2.5	7.8	N
1993	8.1	1.8	1.5	11.4	P
1994	1.3	1.2	1.2	5.9	N
1995	2.8	6.4	13.4	16.5	F, S
1996	1.4	34.6	4.3	9.2	F
1997	2.2	1.9	2.1	9.3	N
1998	3.0	11.8	2.0	22.8	F
1999	7.9	3.6	1.8	10.8	P
2000	2.9	8.2	5.0	10.9	F
2001	1.7	22.7	9.2	48.1	F, S
2002	18.8	12.3	1.5	10.7	P, F
2003	1.1	5.8	2.2	7.9	N
2004	5.2	1.3	1.0	13.1	P
2005	1.2	1.2	1.1	11.5	N
2006	5.7	1.6	1.2	13.0	P
2007	3.0	2.4	34.9	35.0	S
2008	1.4	1.5	2.8	10.1	N
2009	1.6	4.4	22.8	21.2	S
2010	1.1	1.0	1.2	6.1	N
2011	11.8	1.1	1.2	10.8	P
2012	1.1	1.1	1.1	7.0	N

Fig. 5(a) illustrates the identified pluvial floods. We classified seven pluvial flood events considering 5.2-year return period as the minimum threshold level. The region received the highest monsoonal precipitation of 1861.91mm in 2002 leading to an 18.8-year return level of pluvial flood. The highest two precipitation events in 2002 and 2011 caused approximately

11% of total polder area inundation, while 2004 resulted in the highest pluvial inundation (13% area).

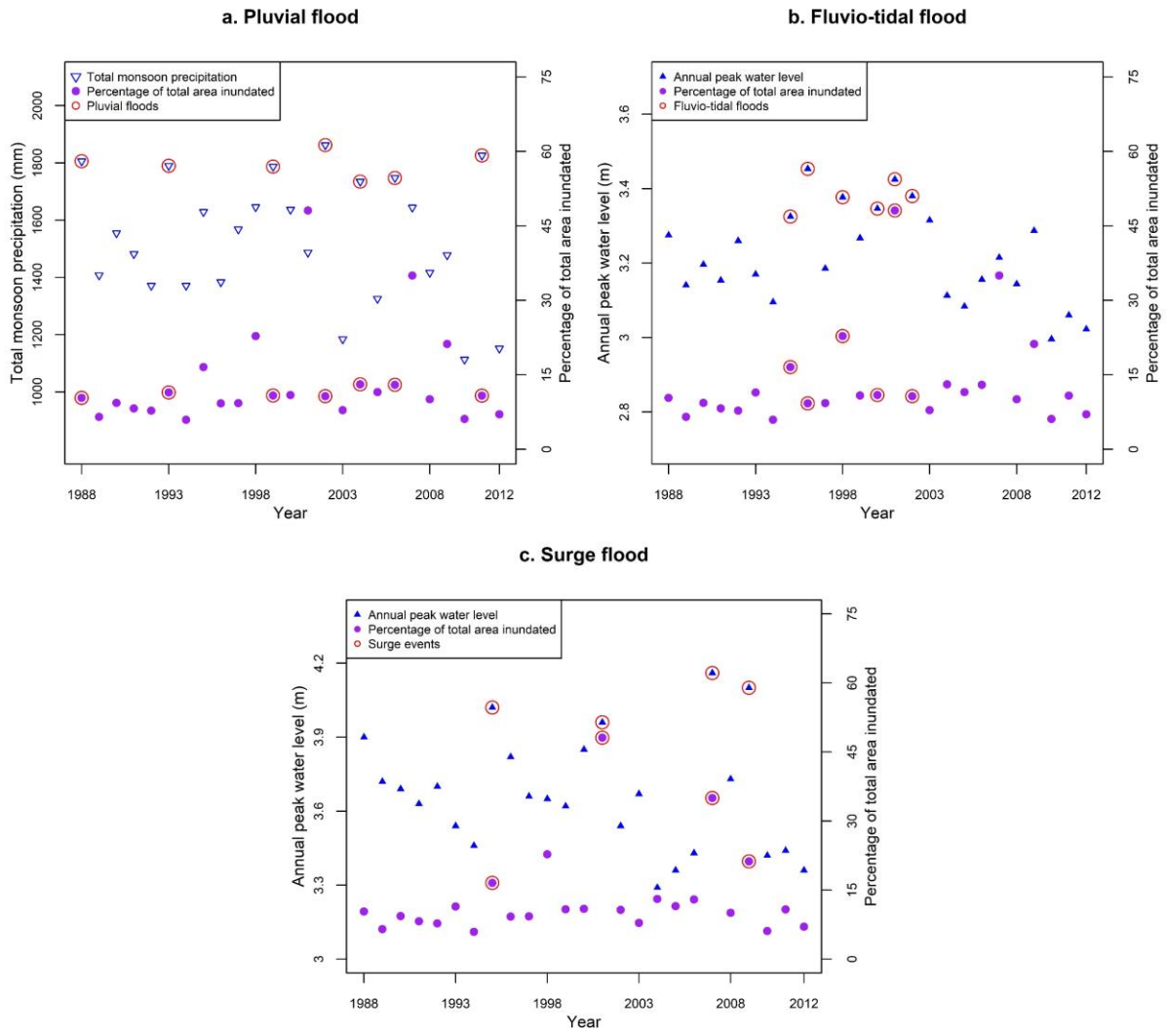

Fig. 5. Classified flood events in relation to values corresponding hydrological parameters.

The six events that were classified as fluvio-tidal happened in 1995, 1996, 1998, 2000, 2001, and 2002. The highest regional average peak water level of 3.45m was observed in 1996, leading to a 34.6-year event (Fig. 5(b)). But the most extreme event did not result in the highest extent of inundation. For instance, whilst in 1996 the inundation area was 9%, the highest percentage of total area (48%) was inundated in 2001 when the region experienced a 23-year fluvio-tidal flood which breached various polders. However, the 2001 event was attributed to both the fluvio-tidal and surge event, though fluvio-tidal flood was the dominant force (as

higher return period) leading to the inundation. Fluvio-tidal floods mostly occurred in between 1995 and 2002. After 2003, relatively a lower mean discharge in upper Ganges River was observed (Figure S6, supplementary document), contributing to a lower peak river water level.

Four surge induced floods were attributed, considering the estimated 7.9-year return period as minimum threshold limit (Fig. 5(c)). The most extreme surge occurred in 2007 during the cyclone Sidr, when the peak surge height reached to 4.16m (35-year return period), causing 35% of the total area inundation. Another major cyclone Aila affected the study area in 2009 with a peak surge of 4.10m, leading to 21% area inundation. Both fluvio-tidal and surge flooding formed the compound event of 1995, when the impact of surge was the highest.

3.3. Modelling flood inundation with and without polders

The outcome of pluvial flood model indicated that the study area was prone to pluvial inundation annually, since excess precipitation of different magnitude was estimated in all studied years (Fig. 6). The extent of inundation has a strong positive correlation with the amount of excess precipitation (correlation coefficient = 0.90). Among the classified seven pluvial flood events (Table 1), the lowest level of monsoon precipitation was observed in 2004. But, the greatest extent of pluvial inundation was estimated in 2004, due to presence of the highest amount of excess precipitation caused by a lower level of evapotranspiration. In 2005, the modelled pluvial inundation was 11.2% area, which is similar to observed flood inundation (11.5%) for that year. The lowest level of evapotranspiration was estimated in 2005, leading to a higher amount of excess precipitation. Therefore, the extent of inundation in 2005 was greater than A_f' (10.3%), despite the region received a 1.2-year return level precipitation. Thus, we included this event to validate the outcome of pluvial flood modelling (Section 2.4.1). The results from pluvial flood modelling further demonstrated that a greater extent of inundation was the outcome of polder construction and inadequate drainage systems. The extent of pluvial inundation would have been substantially lower in absence of polders.

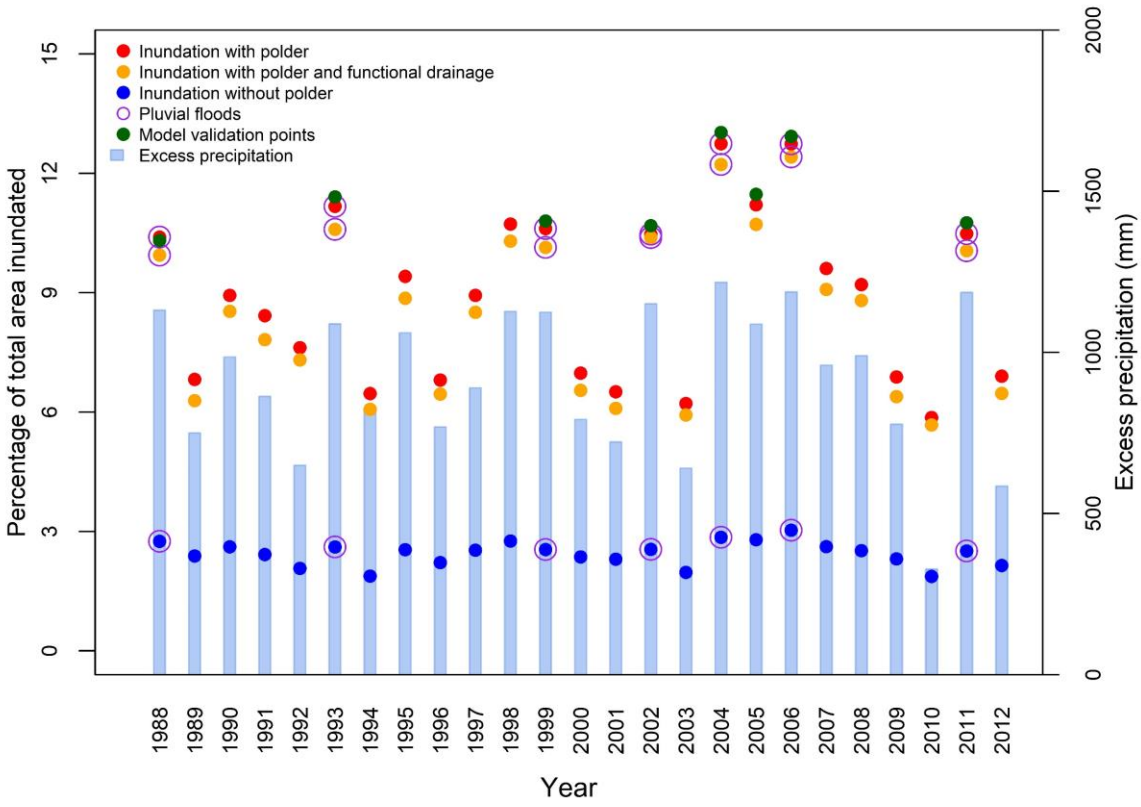

Fig. 6. Simulated pluvial flood inundation for three scenarios.

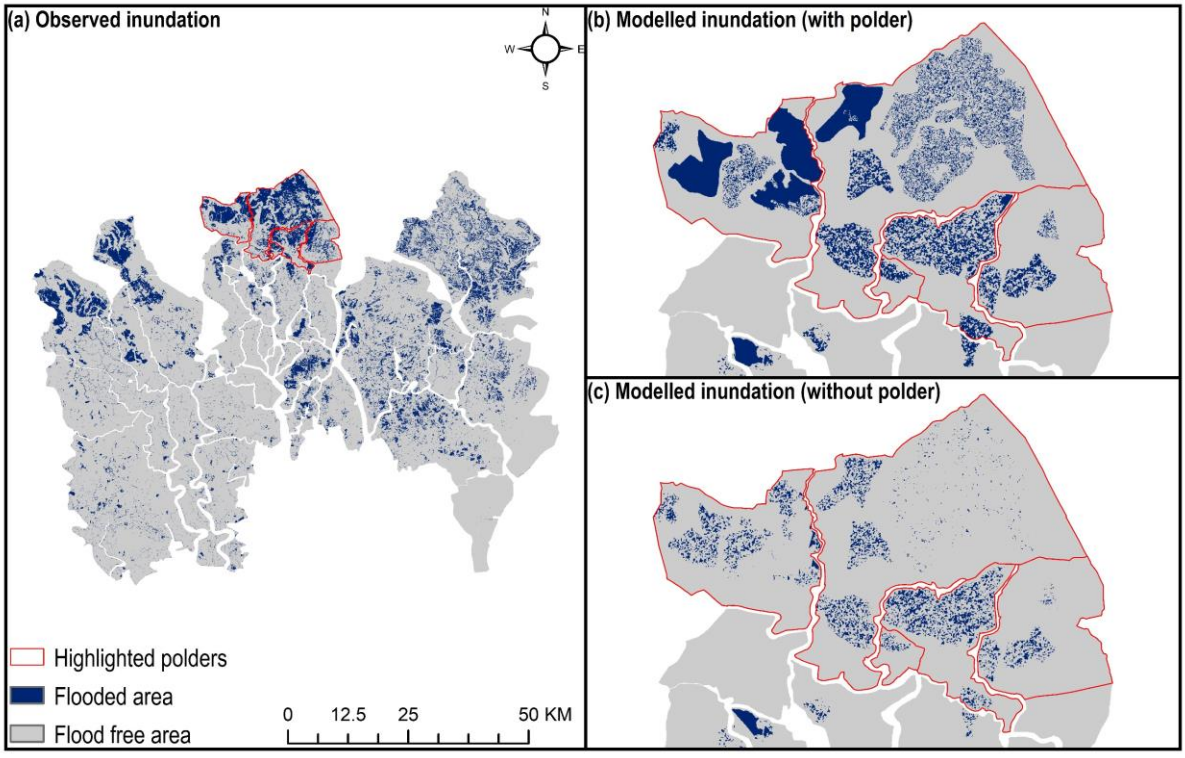

Fig. 7. Impact of polders on pluvial flooding (2004 event).

Typical results from the pluvial flood model are shown in Fig. 7(b, c), which illustrates how a combination of land subsidence (a maximum of approximately 0.5m relative to locations where polders were not constructed) and inadequate drainage, has exacerbated pluvial flooding. We estimate that on average over the modelled period the extent of flooded area was 334km^2 (i.e. 6.5% of total area) larger because of the land subsidence, generated from the construction of polders, and inadequate drainage. The extent of inundation primarily depends on the number of surface depressions generated due to land subsidence. Polder construction increased the number of shallow depressions (<1m in depth), which are prone to flooding. Without polders flooding in those areas might have been alleviated, as sedimentation would have transformed the geomorphology of the region and reduced the number of shallow depressions. Flooding in that case would have only occurred in areas characterized as deep surface depressions. Hence, our modelled pluvial inundation for the counter-factual scenario showed relatively a small year-to-year difference in the extent of inundation (Fig. 6), although the total inundated area was positively correlated with the estimated excess precipitation.

Results from the pluvial flood model further indicated that if the observed drainage system were maintained adequately, it would have been able to reduce pluvial flooding by about 4.9%. This number is relatively small because there are many catchments that were not observed to have a drainage channel. The pluvial flood prone area comprises about 50% aquaculture land (shrimp culture and freshwater fish culture), which is not necessarily harmfully affected by flooding. However, 40% of the flood-prone area is agricultural land (rice field, other croplands, mixed rice and shrimp culture) which can be more adversely impacted by pluvial flooding, whilst 10% is comprised of settlement areas with homestead vegetation where pluvial flooding is directly harmful.

Simulations of fluvio-tidal and surge flooding demonstrate the effectiveness of embankments in reducing inundation due to elevated water levels. For example, during the

1998 fluvio-tidal flood, majority of the region would have been flooded without polders. The presence of polders resulted in an estimated 27% of total area being flooded in this fluvio-tidal flood, compared to 79% for the 'without polder' counter-factual. Complete inundation occurred in 14 polders for 'with' polder scenario, which would have been escalated to 31 polders for the counter-factual scenario (Fig. 8(a)). Overlaying the inundated areas for both scenarios, we found that the embankments protected an estimated 54% area from flooding.

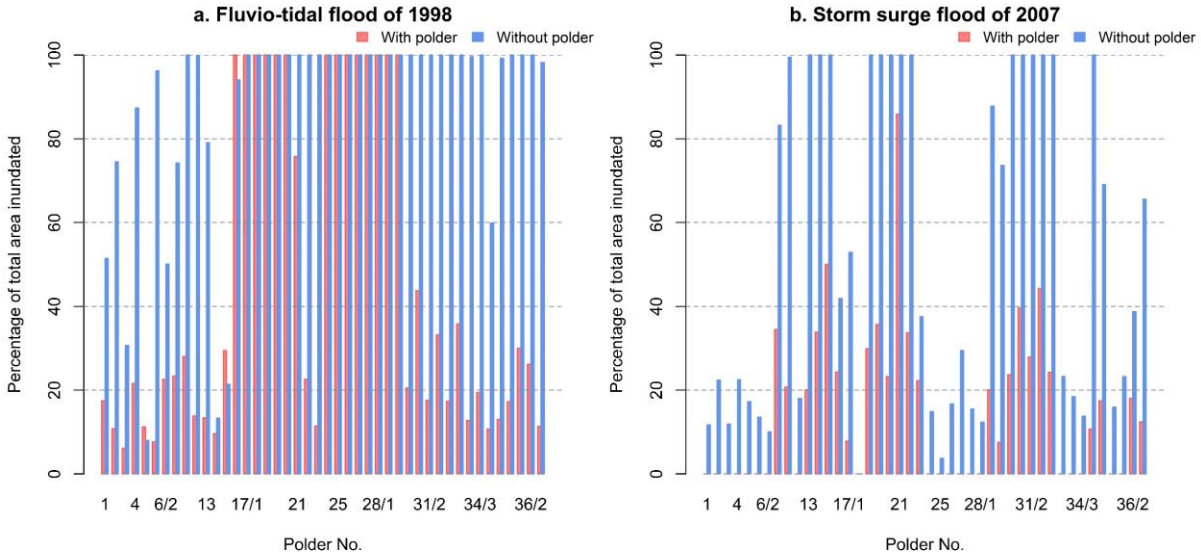

Fig. 8. Polder wise inundation in two scenarios during (a) fluvio-tidal flood of 1998, and (b) storm surge flood of 2007.

Simulation results for surge event Sidr suggests that, in presence of polders (without breaching), about 18% of the total area might have been inundated. Without polders, the extent of inundation would have been increased to approximately 35% area. Seventeen different polders that were partially at risk of flooding would have been inundated by more than 80% area without embankments (Fig. 8(b)). However, our modelled total inundation for counter-factual scenario is similar to the observed inundation of 35% area. When simulating inundation for 'with polder' scenario, the model considered overtopping as the flood mechanism in polders. Therefore, the number of flood-affected polders were substantially lower under this scenario. But, embankment failure in several polders, both in form of damage and overtopping,

increased the extent of inundation. Furthermore, the observed inundation in 2007 is a compound inundation of pluvial and surge induced flooding. The estimated pluvial inundation in 2007 was about 10% area. Subtracting (spatially) the pluvial inundation from the observed inundation, we found that surge induced flood solely contributed to the inundation in 25% area.

4. Conclusion

Creation of polders by construction of embankments in coastal Bangladesh has been a controversial process. The creation of polders enabled large increases in agricultural production and reduced the impacts of storm surges and fluvio-tidal floods. However, blocking off the coastal floodplain from channels practically eliminated annual deposition of sediments on the land, whilst compaction of sediment and anthropogenic activities exacerbated land subsidence. Over the years, drainage channels have not been adequately maintained, which has inhibited drainage of pluvial flood waters and exacerbated inundations. Moreover, construction of polders has provided an impression of security from flood hazards, encouraging human settlement in vulnerable locations.

In this paper we have empirically analysed the evidence for both the beneficial and harmful impacts of polder construction. We found that pluvial flooding occurs frequently, but the flood extent is usually less than in other forms of flooding. By modelling a counter-factual scenario in which polders had not been constructed we quantified a substantial (6.5% area) increase in pluvial flooding that can be attributed to land subsidence resulted from polder construction and poor management of drainage facilities.

On the other hand, the polders have provided protection against fluvio-tidal and storm surge events. In the worst fluvio-tidal flood in the ‘without polder’ scenario 79% of the area would have been flooded, compared with 27% which occurred with the polders. In the surge event Sidr, 18% of the polder area would have been flooded, without the breaching to embankments. But, the extent of inundation was increased to 25% area due to the damage to

embankments during the cyclone. Simultaneously, pluvial flooding exacerbated the flood impact, inundating a total 35% area in 2007.

The empirical analysis of past floods reported in this paper is subject to errors in observations of precipitation and water levels. In addition, the recognition of flooded areas from satellite imagery is also subject to error. The attribution of flood types is to some extent subjective, based on the criteria that were used to optimise the classification thresholds. Given the relatively short record of flood events, the complexity of the flooding process and the possibility of compound events, it would not be possible to establish a definitive classification method.

Flooding processes in low-lying coastal areas are complex, so the modelling we have used to analyse the 'without polder' counter-factual is inevitably approximate. This particularly applies to pluvial flooding, which is sensitivity to local rainfall patterns, topography, land surface and drainage and so would be extremely difficult to model with more accuracy on the spatial/temporal scale considered in this study. Nonetheless, these models have provided insights into the polders' effectiveness. Generally, this study is an attempt to estimate the impact of anthropogenic intervention (creation of coastal embankments) on the hydrology (inundation) of south western embanked region of Bangladesh.

Rehabilitation and reconstruction of embankments is now under way in the coastal zone of Bangladesh (Figure S8, supplementary document). Further choices will need to be made in the face of rising sea levels. Alternative adaptation strategies are being examined as part of the Bangladesh Delta Plan. The empirical analysis of the benefits and impacts of embankment construction, which has been reported in this paper, should help to inform plans for adaptation of Bangladesh's coastal zone to flood hazards, by helping to target and sequence investments for flood management.

Acknowledgement

This work is an output from the REACH programme (www.reachwater.org.uk) funded by UK Aid from the UK Department for International Development (DFID) for the benefit of developing countries (Aries Code 201880). However, the views expressed, and information contained in it are not necessarily those of or endorsed by DFID, which can accept no responsibility for such views or information or for any reliance placed on them. We thank the anonymous reviewers for their careful reading of our manuscript and insightful comments and suggestions.

Appendix A. Supplementary data

Supplementary data to this article can be found online at https://doi.org/10.1016/j.scitotenv.2019.05.04.

5. References

Abdullah AYM, Masrur A, Adnan MSG, Baky MAA, Hassan QK, Dewan A. Spatio-Temporal Patterns of Land Use/Land Cover Change in the Heterogeneous Coastal Region of Bangladesh between 1990 and 2017. Remote Sensing 2019; 11: 790.

Abedin MA, Shaw R. The role of university networks in disaster risk reduction: Perspective from coastal Bangladesh. International Journal of Disaster Risk Reduction 2015; 13: 381-389.

Ahmed KR, Akter S. Analysis of landcover change in southwest Bengal delta due to floods by NDVI, NDWI and K-means cluster with landsat multi-spectral surface reflectance satellite data. Remote Sensing Applications: Society and Environment 2017; 8: 168-181.

Akber MA, Khan MWR, Islam MA, Rahman MM, Rahman MR. Impact of land use change on ecosystem services of southwest coastal Bangladesh. Journal of Land Use Science 2018; 13: 238-250.

Alam MS, Sasaki N, Datta A. Waterlogging, crop damage and adaptation interventions in the coastal region of Bangladesh: A perception analysis of local people. Environmental Development 2017; 23: 22-32.

Auerbach LW, Goodbred SL, Jr., Mondal DR, Wilson CA, Ahmed KR, Roy K, et al. Flood risk of natural and embanked landscapes on the Ganges-Brahmaputra tidal delta plain. Nature Climate Change 2015; 5: 153-157.

Bamberg S, Masson T, Brewitt K, Nemetschek N. Threat, coping and flood prevention – A meta-analysis. Journal of Environmental Psychology 2017; 54: 116-126.

Bhuiyan MJAN, Dutta D. Analysis of flood vulnerability and assessment of the impacts in coastal zones of Bangladesh due to potential sea-level rise. Natural Hazards 2012; 61: 729-743.

Brammer H. Bangladesh's dynamic coastal regions and sea-level rise. Climate Risk Management 2014; 1: 51-62.

Brouwer R, Akter S, Brander L, Haque E. Socioeconomic Vulnerability and Adaptation to Environmental Risk: A Case Study of Climate Change and Flooding in Bangladesh. Risk Analysis 2007; 27: 313-326.

Brown S, Nicholls RJ. Subsidence and human influences in mega deltas: The case of the Ganges–Brahmaputra–Meghna. Science of The Total Environment 2015; 527-528: 362-374.

CEIP. Technical feasibility studies and detailed design for Coastal Embankment Improvement Programme (CEIP). Ministry of Water Resources, Government of the People's Republic of Bangladesh, Dhaka, 2013.

Childs C. Interpolating surfaces in ArcGIS spatial analyst. ArcUser, July-September 2004; 3235: 569.

Choudhury NY, Paul A, Paul BK. Impact of costal embankment on the flash flood in Bangladesh: A case study. Applied Geography 2004; 24: 241-258.

Coles S, Bawa J, Trenner L, Dorazio P. An introduction to statistical modeling of extreme values. Vol 208: Springer, 2001.

Diaz-Nieto J, Lerner DN, Saul AJ, Blanksby J. GIS Water-Balance Approach to Support Surface Water Flood-Risk Management. Journal of Hydrologic Engineering 2011; 17: 55-67.

Dingman SL. Physical hydrology: Waveland Press, 2002.

Falconer R, Cobby D, Smyth P, Astle G, Dent J, Golding B. Pluvial flooding: new approaches in flood warning, mapping and risk management. Journal of Flood Risk Management 2009; 2: 198-208.

Gain AK, Benson D, Rahman R, Datta DK, Rouillard JJ. Tidal river management in the south west Ganges-Brahmaputra delta in Bangladesh: Moving towards a transdisciplinary approach? Environmental Science and Policy 2017; 75: 111-120.

Gilleland E, Katz RW. Extremes 2.0: an extreme value analysis package in r. Journal of Statistical Software 2016; 72: 1-39.

Haque A, Kay S, Nicholls RJ. Present and Future Fluvial, Tidal and Storm Surge Flooding in Coastal Bangladesh. Ecosystem Services for Well-Being in Deltas. Springer, 2018, pp. 293-314.

Haque A, Nicholls RJ. Floods and the Ganges-Brahmaputra-Meghna Delta. Ecosystem Services for Well-Being in Deltas. Springer, 2018, pp. 147-159.

Haque A, Rahman M. Flow Distribution and Sediment Transport Mechanism in the Estuarine Systems of Ganges-Brahmaputra-Meghna Delta. International Journal of Environmental Science and Development 2016; 7: 22.

Hoque R, Nakayama D, Matsuyama H, Matsumoto J. Flood monitoring, mapping and assessing capabilities using RADARSAT remote sensing, GIS and ground data for Bangladesh. Natural Hazards 2011; 57: 525-548.

Houston D, Werritty A, Bassett D, Geddes A, Hoolachan A, McMillan M. Pluvial (rain-related) flooding in urban areas: the invisible hazard. York: Joseph Rowntree Foundation 2011.

Hui R, Jachens E, Lund J. Risk-based planning analysis for a single levee. Water Resources Research 2016; 52: 2513-2528.

Huq M, Khan MF, Pandey K, Ahmed MMZ, Khan ZH, Dasgupta S, et al. Vulnerability of Bangladesh to cyclones in a changing climate: potential damages and adaptation cost: The World Bank, 2010.

Islam M, Kotani K, Managi S. Climate perception and flood mitigation cooperation: A Bangladesh case study. Economic Analysis and Policy 2016a; 49: 117–133.

Islam MA, Mitra D, Dewan A, Akhter SH. Coastal multi-hazard vulnerability assessment along the Ganges deltaic coast of BangladesheA geospatial approach. Ocean & Coastal Management 2016b; 127: 1-15.

Kay S, Caesar J, Janes T. Marine Dynamics and Productivity in the Bay of Bengal. Ecosystem Services for Well-Being in Deltas. Springer, 2018, pp. 263-275.

Kay S, Caesar J, Wolf J, Bricheno L, Nicholls RJ, Saiful Islam AKM, et al. Modelling the increased frequency of extreme sea levels in the Ganges-Brahmaputra-Meghna delta due to sea level rise and other effects of climate change. Environmental Sciences: Processes and Impacts 2015; 17: 1311-1322.

Khan MMH, Bryceson I, Kolivras KN, Faruque F, Rahman MM, Haque U. Natural disasters and land-use/land-cover change in the southwest coastal areas of Bangladesh. Regional Environmental Change 2015; 15: 241-250.

Lillesand T, Kiefer RW, Chipman J. Remote sensing and image interpretation: John Wiley & Sons, 2014.

Masud MMA, Moni NN, Azadi H, Van Passel S. Sustainability impacts of tidal river management: Towards a conceptual framework. Ecological Indicators 2018; 85: 451-467.

McHugh ML. Interrater reliability: the kappa statistic. Biochemia Medica 2012; 22: 276-282.

Moniruzzaman M. Impact of Climate Change in Bangladesh: Water Logging at South-West Coast. In: Leal Filho W, editor. Climate Change and the Sustainable Use of Water Resources. Springer Berlin Heidelberg, Berlin, Heidelberg, 2012, pp. 317-336.

Mukhopadhyay A, Hornby DD, Hutton CW, Lázár AN, Amoako Johnson F, Ghosh T. Land Cover and Land Use Analysis in Coastal Bangladesh. In: Nicholls RJ, Hutton CW, Adger WN, Hanson SE, Rahman MM, Salehin M, editors. Ecosystem Services for Well-Being in Deltas: Integrated Assessment for Policy Analysis. Springer International Publishing, Cham, 2018, pp. 367-381.

Nied M, Pardowitz T, Nissen K, Ulbrich U, Hundecha Y, Merz B. On the relationship between hydro-meteorological patterns and flood types. Journal of Hydrology 2014; 519: 3249-3262.

Nishat A, Nishat B, Abdullah Khan MF. A Strategic View of Land Management Planning in Bangladesh. Flood Risk Science and Management, 2010, pp. 484-498.

Nowreen S, Jalal MR, Khan MSA. Historical analysis of rationalizing South West coastal polders of Bangladesh. Water Policy 2014; 16: 264-279.

Paul BK, Rashid H. Climatic Hazards In Coastal Bangladesh - Non-Structural and Structural Solutions. Cambridge, United States: Elsevier, 2017.

Raber GT, Jensen JR, Hodgson ME, Tullis JA, Davis BA, Berglund J. Impact of LiDAR nominal post-spacing on DEM accuracy and flood zone delineation. Photogrammetric engineering & remote sensing 2007; 73: 793-804.

Rahman R, Salehin M. Flood Risks and Reduction Approaches in Bangladesh. In: Shaw R, Mallick F, Islam A, editors. Disaster Risk Reduction Approaches in Bangladesh. Springer, Tokyo, 2013, pp. 65-90.

Rao AR, Hamed K. Flood frequency analysis. USA: CRC press, 2000.

Roy K, Gain AK, Mallick B, Vogt J. Social, hydro-ecological and climatic change in the southwest coastal region of Bangladesh. Regional Environmental Change 2017; 17: 1895-1906.

Sanyal J, Lu XX. Application of remote sensing in flood management with special reference to monsoon Asia: A review. Natural Hazards 2004; 33: 283-301.

Sarp G, Ozcelik M. Water body extraction and change detection using time series: A case study of Lake Burdur, Turkey. Journal of Taibah University for Science 2017; 11: 381-391.

Seibert J, McGlynn BL. A new triangular multiple flow direction algorithm for computing upslope areas from gridded digital elevation models. Water Resources Research 2007; 43.

Singh RK, Hari Prasad V, Bhatt CM. Remote sensing and GIS approach for assessment of the water balance of a watershed. Hydrological Sciences Journal 2004; 49: 131-142.

Talchabhadel R, Nakagawa H, Kawaike K. Tidal River Management (TRM) and Tidal Basin Management (TBM): A case study on Bangladesh. E3S Web of Conferences. 7, 2016.

Tareq SM, Tauhid Ur Rahman M, Zahedul Islam AZM, Baddruzzaman ABM, Ashraf Ali M. Evaluation of climate-induced waterlogging hazards in the south-west coast of Bangladesh using Geoinformatics. Environmental Monitoring and Assessment 2018; 190: 230.

Thornthwaite CW, Mather JR. Instructions and tables for computing potential evapotranspiration and the water balance. Drexel Institute of Technology, Centerton, NJ (EUA). Laboratory of Climatology, 1957.

Van Staveren MF, Warner JF, Khan MSA. Bringing in the tides. from closing down to opening up delta polders via Tidal River Management in the southwest delta of Bangladesh. Water Policy 2017; 19: 147-164.

WARPO. National Water Resources Database(NWRD). Water Resources Planning Organization (WARPO), Bangladesh, 2018.

Xu H. Modification of normalised difference water index (NDWI) to enhance open water features in remotely sensed imagery. International Journal of Remote Sensing 2006; 27: 3025-3033.